

Technical Report

An Alternative Method for Quantitative Mass Spectrometry Imaging (*q*-MSI) of Dopamine Utilizing Fragments of Animal Tissue

Erika Nagano¹, Kazuki Odake¹, and Shuichi Shimma^{*1,2}

¹Research and Development Division, Miruion Corporation, Ibaraki, Osaka 567-0085, Japan

²Department of Biotechnology, Graduate School of Engineering, Osaka University, Suita, Osaka 565-0871, Japan

Mass spectrometry imaging (MSI) is a well-known method for the ionization of molecules on tissue sections and the visualization of their localization. Recently, different sample preparation methods and new instruments have been used for MSI, and different molecules are becoming visible. On the other hand, although several quantification methods (*q*-MSI) have been proposed, there is still room for the development of a simplified procedure. Here, we have attempted to develop a reproducible and reliable quantification method using a calibration curve prepared from tissue debris of a frozen section of a sample when we trim the frozen blocks. We discuss the reproducibility of this method across different sample lots and the effect of the biological matrix (ion suppression) on our results. The quantitative performance was evaluated in terms of accuracy and relative standard deviation, and the reliability of the quantitative values obtained by matrix-assisted laser desorption/ionization-MSI was further evaluated by enzyme-linked immunosorbent assay (ELISA). Our *q*-MSI method for the quantification of dopamine in mouse brain tissue was found to be highly linear, accurate, and precise. The quantitative values obtained by MSI were found to be highly comparable (>85% similarity) to the results obtained by ELISA from the same tissue extracts.



Copyright © 2023 Erika Nagano, Kazuki Odake, and Shuichi Shimma. This is an open-access article distributed under the terms of Creative Commons Attribution Non-Commercial 4.0 International License, which permits use, distribution, and reproduction in any medium, provided the original work is properly cited and is not used for commercial purposes.

Please cite this article as: Mass Spectrom (Tokyo) 2023; 12(1): A0128

Keywords: mass spectrometry imaging, quantitation, *q*-MSI, dopamine, mimic model

(Received May 2, 2023; Accepted July 4, 2023; advance publication released online July 20, 2023)

INTRODUCTION

Mass spectrometry imaging (MSI) using matrix-assisted laser desorption/ionization (MALDI) was first reported in 1997 as a new molecular visualization method using mass spectrometry.¹⁾ MSI has been developed as a technique to visualize various biomolecules by applying new mass spectrometry instruments and sample preparation methods to MSI.

On the other hand, various methods for quantification in MSI have been reported. (1) Spotting a standard of known concentration on a sample plate. (2) Spotting a standard of known concentration on a control tissue section.²⁻⁷⁾ (3) A method of preparing two serial sections of a sample, one measured by MSI and the other with the extracted liquid by liquid chromatography-mass spectrometry (LC-MS/MS)⁸⁻¹⁶⁾ or gas chromatography-coupled mass spectrometry (GC-MS).¹⁷⁾ (4) A method in which standards are added to tissue homogenates and frozen blocks are prepared, followed by the same pretreatment as for real samples.¹⁸⁻²²⁾ (5) The method is the same pretreatment as that for the real samples, after

spiking the powdered frozen tissue with the reference material and preparing a frozen block.²³⁾

While method (1) is extremely simple, it is rarely used because it does not take into account the difference in ionization efficiency between the tissue and the sample plate and the effect of the biological matrix. The disadvantage of (2) is that the accuracy of the calibration curve is poor because the effect of the matrix effect differs even on the same tissue.²⁴⁾ Furthermore, it does not take into account the extraction efficiency of the molecule to be quantified from the tissue. (3) is a combination of distribution information obtained by MSI and quantitative information obtained by existing LC-MS/MS, and is considered to be highly accurate. In method (4), which has already been reported,²²⁾ the tissue is made into a liquid state using an ultrasonic homogenizer. Since the obtained homogenate is extremely viscous, it is difficult to make the tissue homogeneous with the reference material, and the reproducibility of the mimic tissue itself is poor. In addition, the addition of water to reduce the viscosity may cause ice crystals to form inside the tissue after refreezing, making it difficult to cut the tissue into thin slices.

*Correspondence to: Shuichi Shimma, Department of Biotechnology, Graduate School of Engineering, Osaka University, Suita, Osaka 565-0871, Japan, e-mail: sshimma@bio.eng.osaka-u.ac.jp

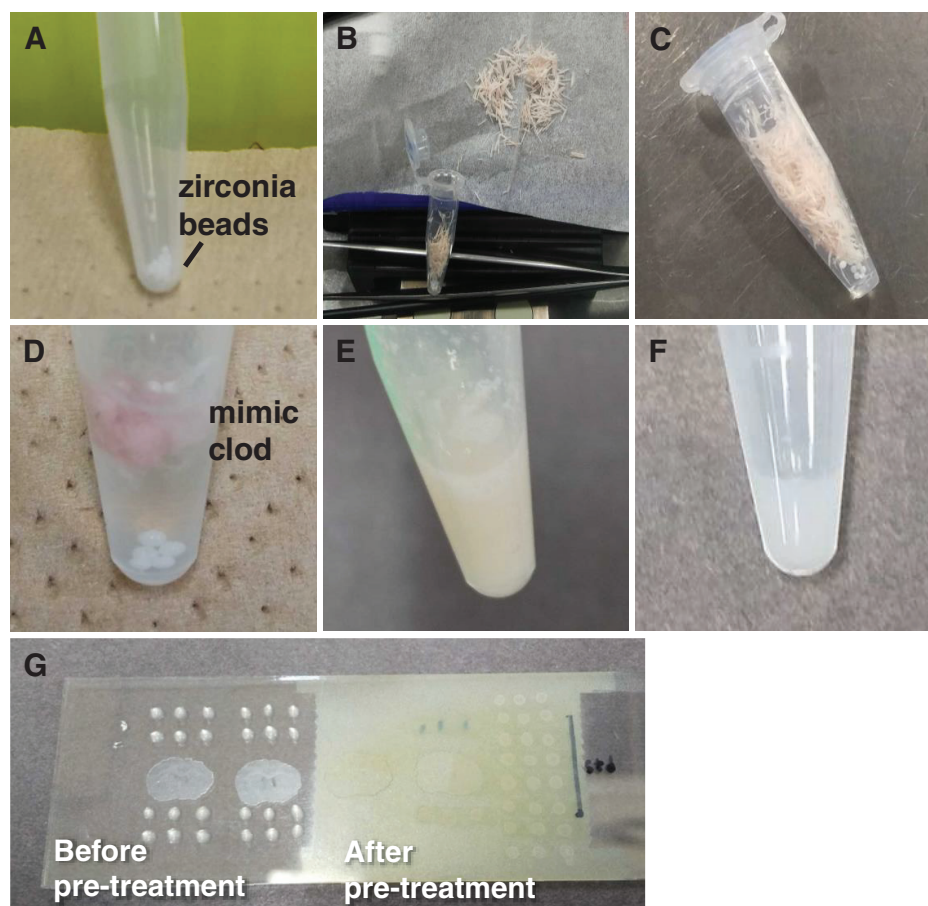


Fig. 1. Sample preparation protocol. (A) Weigh zirconia beads in a 1.5-mL tube. (B) Collect the trimmed pieces. (C) Weigh the collected trimmed pieces. (D) Add 50 μL of ultrapure water to 10 mg of trimmed pieces. (E) Mimic tissue after mixing with a vortex mixer. (F) Mixture of mimic tissue and standard solution. (G) 0.5 μL spot on ITO glass (left), after derivatization reagent and matrix sprayed with an airbrush (right). ITO, indium-tin-oxide.

The reproducibility of (5) is considered to be high because of the high homogeneity of the target molecules inside the mimic tissue. The only issue is the large amount of tissue required.

In this paper, we introduce a simpler and more reproducible alternative method for quantification using mimic tissue. The target was dopamine, a neurotransmitter in the brain. Mouse brains were used. To confirm our reliability, we performed a comparison of dopamine concentration between the *q*-MSI result and the enzyme-linked immunosorbent assay (ELISA) result.

MALDI-MSI allows the imaging of region-specific distributions in tissues. The method we have developed also allows the accurate quantification of molecules distributed in the tissue. This can be used as a tool to understand which regions of the brain dopamine are working and to what extent it is fluctuating, which could be useful for understanding brain disorders and developing drugs.

EXPERIMENTAL

Chemicals and reagents

Frozen mouse brain tissue blocks were purchased from Funakoshi (Tokyo, Japan). Dopamine hydrochloride (DA) for use as standard, 2,5-dihydrobenzoic acid (DHB, 98% purity), 2,4,6-triphenylpyrylium tetrafluoroborate (TPP), and polyethylene glycol 300 were purchased from Merck (Darmstadt, Germany). Dopamine-d4 hydrochloride (DA-d4) for use as an internal standard (IS) (Supporting information, Fig. S1; all

supplementary files are available online.) was purchased from Toronto Research Chemicals (Toronto, ON, Canada). All solvents used in this experiment were of LC-MS grade and purchased from Fujifilm Wako Pure Chemical Industries, Ltd. (Osaka, Japan).

Tissue preparation

An optimal cutting temperature (OCT) compound was used to fix each tissue block on a holder of a cryomicrotome. The frozen tissue block was placed on the surface of the OCT compound and stored at -80°C for 5 min. Frozen 8- μm sections were sliced at -20°C with the cryomicrotome (Leica CM 1950; Leica Microsystems, GmbH, Nussloch, Germany). We used a block of three mice of the wild-type (C57BL/6J). Sections for MSI were collected for each individual in the striatum (*St*) area. The frozen sections were thaw mounted on an indium-tin-oxide-coated glass slide (SI0100N; Matsunami, Osaka, Japan) and allowed to dehydrate in a 50-mL conical tube containing silica gel. The glass slides were stored at -20°C in the tube until matrix application.

Mimic tissue preparation

The general flow is shown in Fig. 1. Zirconia beads (1 mm diameter) were placed in a 1.5 mL tube and weighed. For three mice, trimming debris from frozen sections including the cerebral cortex (*Cc*) was collected, trimmed to cover the entire brain region, and weighed (Fig. 1A-1C). To 10 mg

of the trimmed debris, 50 μ L of water was added (Fig. 1D), and the mixture was prepared with a vortex mixer (Fig. 1E). The homogenate solution was used as a mimic sample, and the mimic sample was mixed with the standard solution at a ratio of 1 : 1 (v/v) (Fig. 1F). In this experiment, 10 mg/mL of aqueous DA solution was prepared as the stock solution. Standard solutions were prepared from the stock solutions by using ultrapure water as a solvent, and the mimic samples for the calibration curve were prepared so that the final DA concentrations mixed with the mimic samples were 0, 5, 10, 20, 50, and 75 μ g/g. 0.5 μ L of the mixture was dropped onto an indium–tin–oxide (ITO) glass slide and allowed to dry (Fig. 1G).

Derivatization

Derivatization is essential for the detection of DA using MALDI-MSI. The derivatization method was adapted from a previously reported method using TPP as the derivatization reagent.^{25,26} The TPP stock solution was prepared to 6 mg/mL using methanol as the solvent. TPP stock solution was diluted to 1 mg/mL using methanol : ultrapure water : triethylamine (8 : 2 : 0.6, v/v) as a dilution solvent, and this was used as the derivatization reagent solution.

Derivatization of DA standard solutions and mimic samples was performed by spotting on ITO glass. Derivatization of DA in mouse brain for MALDI-MSI was performed on 8- μ m thick coronal sections. For quantification, derivatization was performed using an airbrush (HT-381 0.3 cm; WAVE, Tokyo, Japan) by uniformly spraying 300 μ L of reagent solution onto one mouse brain section and a calibration curve prepared from three different mouse brains. Each sample was used to prepare samples without and with ISS. After spraying, the derivatization reaction was allowed to stand at room temperature (approximately 25°C) for 1 hour to complete the derivatization reaction on the tissue. For the IS method, the IS (DA-d4) solution dissolved in methanol was diluted with TPP solution to a final concentration of 1 μ g/mL. DA-d4 was derivatized for 5 min at room temperature. The derivatization TPP-DA-d4 solution was applied over 300 μ L/slide (one section and the calibration curve) with the airbrush.

MALDI matrix supply

After completion of the derivatization reaction on the tissue, the MALDI matrix was immediately supplied onto the tissue. In this experiment, DHB was used as the MALDI matrix (Fig. S2) and was supplied using an airbrush. A total of 30 mg/mL of DHB solution was added to methanol : ultrapure water (1 : 1, v/v) as a solvent, and trifluoroacetic acid was added to achieve a final concentration of 0.1%. The DHB solution was mixed with a vortex mixer and sonicated for 5 min, and the supernatant was used for spraying. After spraying the matrix solution, the samples were allowed to stand at room temperature for 10 min before measurement. To prevent contamination during the matrix spraying process, a different airbrush was used for spraying the derivatization reagent and the matrix solution.

MALDI-MSI analysis

MALDI-MSI experiment was performed on a MALDI ion trap time-of-flight mass spectrometer (iMScope TRIO; Shimadzu, Kyoto, Japan).²⁷ The laser diameter was 25 μ m. Data were collected at 100- μ m intervals. The tissue surface was laser irradiated with 100 shots (1 kHz repetition rate) for each pixel. All the data were acquired in the positive-ion

detection mode using an external calibration method. Since the transition of m/z 444.19 \rightarrow 308.14 was monitored, the data acquisition parameters of laser power and collision energy were adjusted to 70% and 50 (dimensionless collision energy in iMScope TRIO), respectively, to obtain the maximum intensity at m/z 308.14. The voltage of the microchannel plate detector was 2.1 kV. After sample analysis, the ion images were reconstructed based on data extracted from m/z ranges of the target $m/z \pm 0.03$ Da using Imaging MS Solution (Shimadzu). Signal intensities from the region of interest were extracted using an Imaging MS Solution. MS images acquired from measurements using IS were obtained by calculating TPP-DA/TPP-DA-d4 using IMAGEREVEAL (Shimadzu).

Validity of the calibration curve

Calibration curves were assessed for relative standard error (RSD) and accuracy. The formula is based on the “bioanalytical method validation and study sample analysis (ICH-M10).”

$$\text{RSD (\%)} = (\text{standard deviation/mean value}) \times 100$$

$$\text{Accuracy (\%)} = (\text{measured value/theoretical value}) \times 100$$

ELISA

DA was extracted from mouse brain sections and quantified in the *St* of the mouse brain by ELISA using a DA ELISA kit (ImmuSmol SAS, Bordeaux, France). A microplate reader SH-9000Lab (Hitachi, Tokyo, Japan) was also used for absorbance (450–650 nm) measurement. This ELISA kit is a competitive ELISA. Two-dimensional fitting was used because it is generally recommended to use a four-parameter logistic curve, as the competing method results in an inverse sigmoid curve.

Hematoxylin and eosin (HE) stain

We performed staining with Meyer’s hematoxylin solution for 1 min. After that, the samples were lightly rinsed with water, and washed with fresh water for 1 min. It was then immersed in a 1% solution of eosin Y for 4 sec and washed as described above. Dehydration was followed by three soaks in 100% ethanol for 1 min, followed by two permeations in 100% xylene for 1 min. After the permeation process, the sections were placed on anti-exfoliation-coated glass slides (Matsunami Glass Industry, Osaka, Japan) with the sections facing up, sealed with a passomount (sealing glue), placed on a coverslip (Matsunami Glass Industry), and left to dry overnight. The images were taken using an all-in-one microscope (Keyence, Osaka, Japan).

RESULTS AND DISCUSSION

Imaging of DA in mouse brain section

TPP-DA product ion spectra from the mouse brain section are shown in Fig. 2A. This spectrum was identical to the TPP-DA spectrum obtained by derivatization of the DA standard solution. From this spectrum, it can be seen that the obtained TPP-DA is characterized by the detection of m/z 308.14 derived from the TPP reagent side. Imaging of TPP-DA in coronal sections of frozen mouse brain tissue is shown in Fig. 2B. Compared with the results of HE staining of the sections after MSI measurement, the distribution of TPP-DA appears to be localized in the *St*. This distribution reproduces the previously reported results.²² We have attempted to improve the TPP-DA peak intensity by examining the derivatization conditions (Fig. S3). At room temperature (25°C), the TPP-DA spectral intensity remained the same regardless of

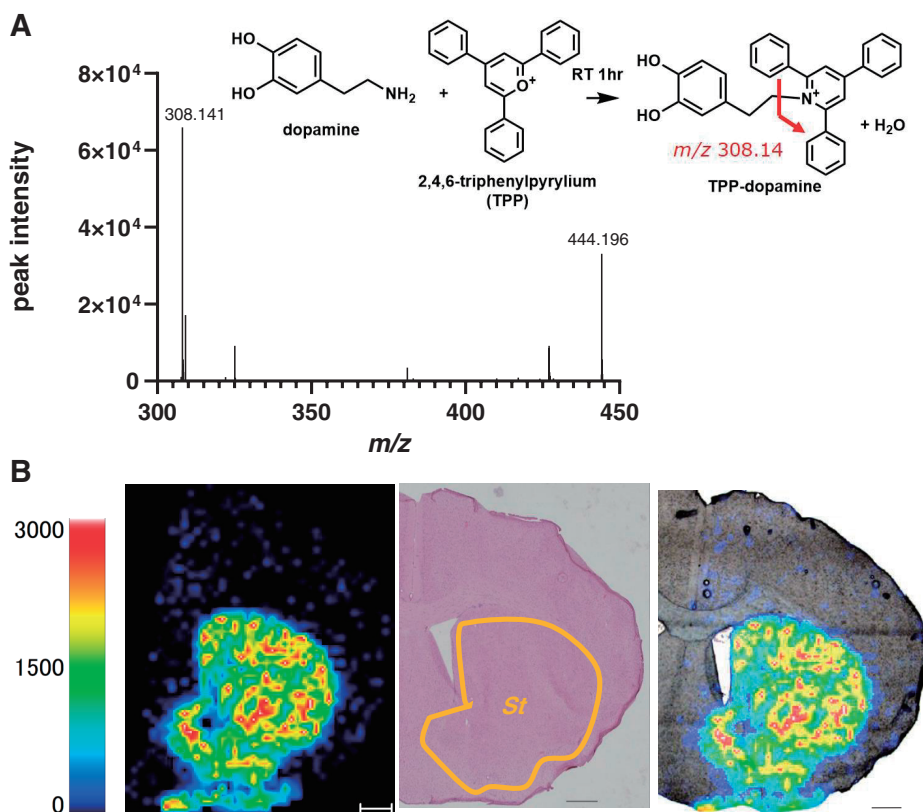


Fig. 2. (A) Molecular structure and mass spectrum of TPP-DA produced by the reaction of TPP and DA. m/z 308.14 is the MSMS spectrum of TPP-DA and m/z 442.19 is the MS spectrum of TPP-DA. (B) Distribution of TPP-DA in coronal sections of mouse brain tissue. Compared with HE staining of post-measured sections. The scale bar is 500 μm . DA, dopamine hydrochloride; HE, hematoxylin and eosin; MS, mass spectrometry; St, striatum; TPP, triphenylpyrylium tetrafluoroborate.

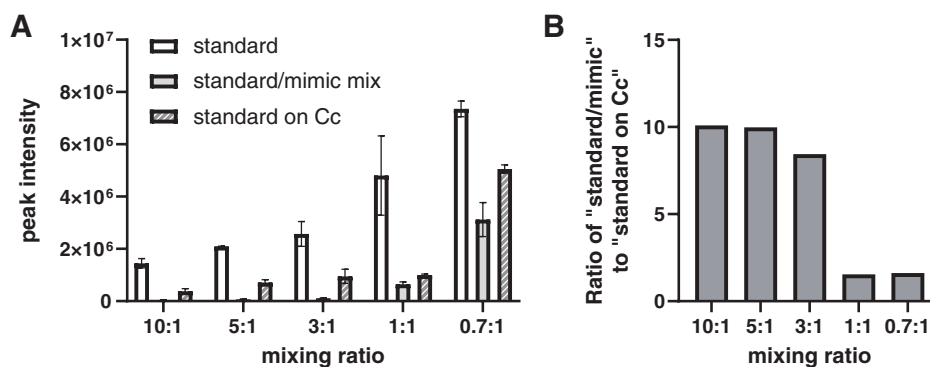


Fig. 3. Influence of matrix in vivo. The standard solution was spotted on ITO glass (standard), a mixture of standard and mimic tissue mix was spotted on ITO glass (standard/mimic mix), and the standard solution was spotted on a section of Cc (standard on Cc). For standard and standard on Cc, standard solutions were prepared in ultrapure water to have the same final concentration as that of standard/mimic mix. "Standard" and "standard on Cc" indicate the ratio of water : standard solution; "standard/mimic mix" indicates the ratio of mimic sample : standard solution. (A) Differences in TPP-DA peak intensity for each sample according to the mixing ratio. (B) Ionic strength ratio of standard/mimic mix to standard on Cc. Cc, cerebral cortex; DA, dopamine hydrochloride; ITO, indium-tin-oxide; TPP, triphenylpyrylium tetrafluoroborate.

the amount of TPP. This result indicates that the derivatization reaction in this paper is sufficient. Although the TPP-DA spectral intensity increased with heating (60°C), no quantification by heating was performed in this paper to avoid the influence of heating on the tissue.

Effects of biological matrix

The peak intensities at m/z 308.14 obtained by spotting standard solutions on ITO glass (standard), spotting a mixture of mimic sample and standard solutions on ITO glass

(standard/mimic mix), and spotting standard solutions on sections of mouse brain including Cc were compared (Fig. 3). The detailed numbers are shown in Table 1. The peak at m/z 308.14 was not detected when the matrix solution was spotted on Cc sections. It was therefore used as a control region. For standard and standard on Cc, standard solutions were prepared in ultrapure water to have the same final concentration as that of the standard/mimic mix. The peak intensity of the standard/mimic mix and standard on Cc was clearly lower than that of the standard solution alone when the

Table 1. Peak intensity ratio of mimic/standard mix to standard on Cc. We investigated the mixing ratio of the mimic/standard solution that would result in similar ionization efficiencies for the tissue and the mimic sample.

Mixing ratio	Ratio of "standard/mimic mix" to "standard on brain"
10 : 1	10.10
5 : 1	9.98
3 : 1	8.44
1 : 1	1.54
2 : 1	1.62

Cc, cerebral cortex.

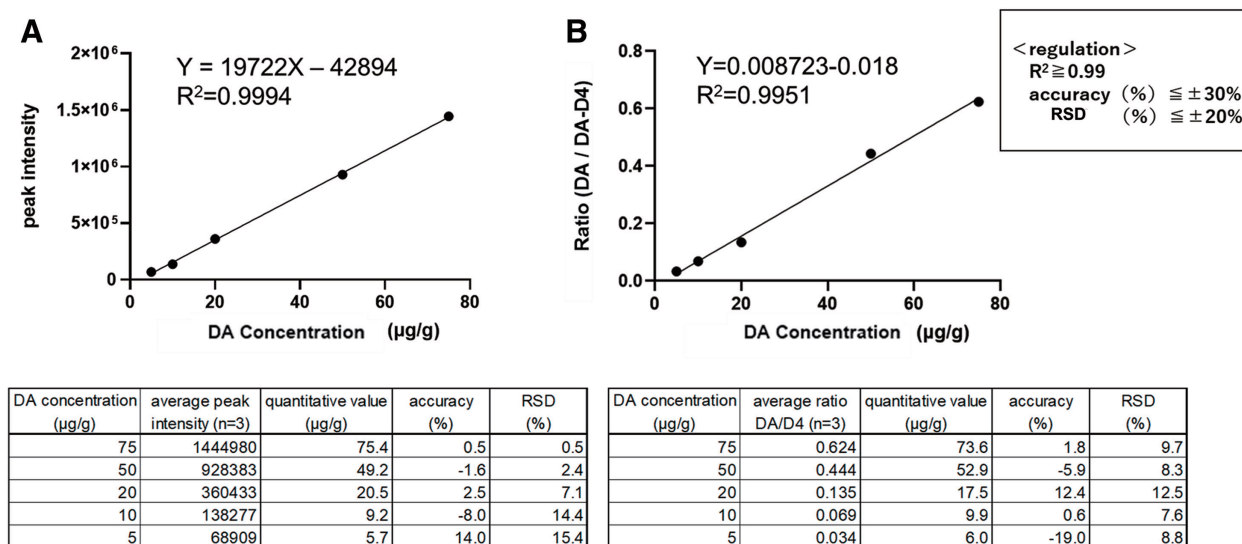


Fig. 4. Evaluation of TPP-DA calibration curves using mimic tissue. (A) Without IS. (B) With IS. DA, dopamine hydrochloride; DA-d4, dopamine-d4 hydrochloride; IS, internal standard; RSD, relative standard deviation; TPP, triphenylpyrylium tetrafluoroborate.

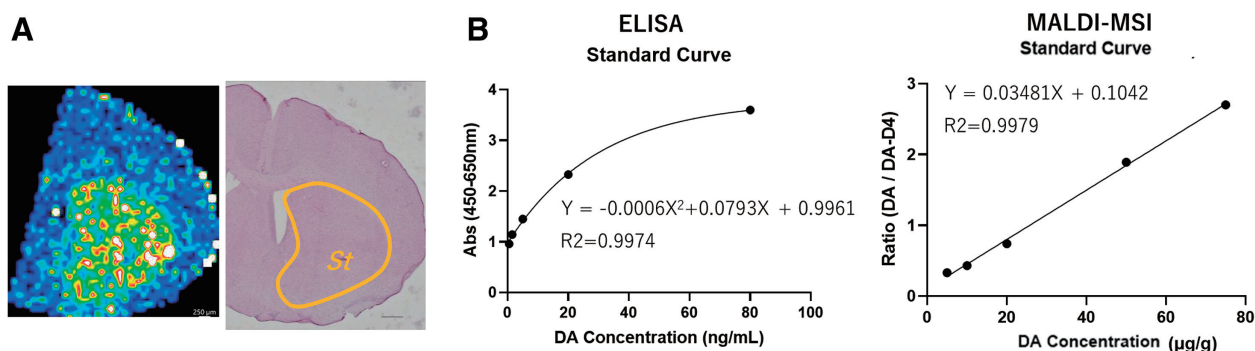


Fig. 5. MSI results and TPP-DA determination in mouse brain *St*. DA-d4 was used as the IS for DA. (A) MSI results are MS images obtained after the calculation of TPP-DA/TPP-DA-d4 using the analysis software IMAGEREVEAL (Shimazu, Kyoto, Japan). (B) Quantitative values for ELISA kits. This ELISA kit is a competitive ELISA. Two-dimensional fitting was used because it is generally recommended to use a four-parameter logistic curve, as the competing method results in an inverse sigmoid curve. (C) Quantitative values for MALDI-MSI with IS. DA, dopamine hydrochloride; DA-d4, dopamine-d4 hydrochloride; ELISA, enzyme-linked immunosorbent assay; IS, internal standard; MALDI, matrix-assisted laser desorption/ionization; MS, mass spectrometry; MSI, mass spectrometry imaging; *St*, striatum; TPP, triphenylpyrylium tetrafluoroborate.

standard solution was spotted on the ITO glass. This result found the influence of the biological matrix (ion suppression). When equal amounts of mimic tissue and standard solution were mixed, there was little difference in peak intensity compared to when the standard solution was spotted on Cc sections (Fig. 3). These results indicate that this method takes into account the influence of the biological matrix, the ionization efficiency on the tissue, and the extraction efficiency of DA in the tissue.

Quantitative MSI of DA in mouse brain *St*

The calibration curve obtained by this method is shown in Fig. 4. We used DA-d4 as the IS for DA. Figure 4A shows the calibration curve for the absolute quantification method without IS, while Fig. 4B shows the calibration curve for the IS method with IS. Calibration curves with $R^2 > 0.99$ were obtained with and without ISs.

MSI results are obtained after the calculation of TPP-DA/TPP-DA-d4 (Fig. 5A). The use of TPP-DA-d4, which has the

Table 2. Quantitative values for ELISA kits and MALDI-MSI. Reproducibility of quantification was checked. Two samples (two mice) were assayed; the accuracy of the quantitative values by MALDI-MSI was assessed using the quantitative values by ELISA as true values.

Sample	DA concentration ($\mu\text{g/g}$)		Accuracy (%)
	ELISA	MALDI-MSI	
1	7.8	6.5	10.7
2	11.1	13.0	10.6

DA, dopamine hydrochloride; ELISA, enzyme-linked immunosorbent assay; MALDI, matrix-assisted laser desorption/ionization, MSI, mass spectrometry imaging.

same ionization efficiency as TPP-DA, the distribution of TPP-DA can be imaged, taking into account differences in ionization efficiency between tissue regions, and shows that TPP-DA is localized to *St*.

The calibration curve with $R^2 > 0.99$ was obtained from the ELISA and MALDI-MSI calibration curves shown in Fig. 5B. This calibration curve was used for quantification. The quantitative value of TPP-DA localized in *St* was 13.0 $\mu\text{g/g}$. The reliability of the quantitative value obtained by MALDI-MSI was evaluated by ELISA and was 11.1 $\mu\text{g/g}$. The similarity with ELISA was more than 85%, indicating the high reliability of this method using MALDI-MSI. The validity of the calibration curve was assessed in terms of RSD and accuracy (Table 2). The coefficient of determination of linearity (R^2) was set to be greater than 0.99, accuracy to be within $\pm 30\%$, and RSD to be within $\pm 20\%$ in MALDI-MSI.

The method can also be used to quantify TPP- γ -amino-butyric acid, one of the neurotransmitters (Figs. S4 and S5), showing that it is a versatile method. The calibration curve with high linearity was obtained even without the IS. The quantitative value obtained by this method is 1361.7 $\mu\text{g/g}$ in the hypothalamus.

CONCLUSION

In this study, we improve upon previously reported quantitative mass imaging methods and develop a simpler, more valid, and reliable quantitative method. The method we developed can generate an excellent calibration curve from the same sample as the one to be quantified, is simpler to investigate, and does not require special equipment compared with conventional methods, thus reducing cost and time.

ACKNOWLEDGMENT

The authors would like to thank the Center for Medical Research and Education at Osaka University for the use of the microplate reader.

REFERENCES

- 1) R. M. Caprioli, T. B. Farmer, J. Gile. Molecular imaging of biological samples: Localization of peptides and proteins using MALDI-TOF MS. *Anal. Chem.* 69: 4751–4760, 1997.
- 2) P. Källback, A. Nilsson, M. Shariatgorji, P. E. Andren. msIQuant—quantitation software for mass spectrometry imaging enabling fast access, visualization, and analysis of large data sets. *Anal. Chem.* 88: 4346–4353, 2016.
- 3) W. Nie, Q. Lu, T. Hu, M. Xie, Y. Hu. Visualizing the distribution of curcumin in the root of *Curcuma longa* via VUV-postionization mass spectrometric imaging. *Analyst (Lond.)* 148: 175–181, 2022.
- 4) W. Tang, J. Chen, J. Zhou, J. Ge, Y. Zhang, P. Li, B. Li. Quantitative MALDI imaging of spatial distributions and dynamic changes of tetrandrine in multiple organs of rats. *Theranostics* 9: 932–944, 2019.
- 5) M. Lagarrigue, R. Lavigne, E. Tabet, V. Genet, J. P. Thome, K. Rondel, B. Guevel, L. Multigner, M. Samson, C. Pineau. Localization and in situ absolute quantification of chlordecone in the mouse liver by MALDI imaging. *Anal. Chem.* 86: 5775–5783, 2014.
- 6) J. G. Swales, A. Dexter, G. Hamm, A. Nilsson, N. Strittmatter, F. Michopoulos, C. Hardy, P. Morentin-Gutierrez, M. Mellor, P. E. Andren, M. R. Clench, J. Bunch, S. E. Critchlow, R. J. A. Goodwin. Quantitation of endogenous metabolites in mouse tumors using mass-spectrometry imaging. *Anal. Chem.* 90: 6051–6058, 2018.
- 7) F. Dewez, E. De Pauw, R. M. A. Heeren, B. Balluff. Multilabel per-pixel quantitation in mass spectrometry imaging. *Anal. Chem.* 93: 1393–1400, 2021.
- 8) K. Hattori, M. Kajimura, T. Hishiki, T. Nakanishi, A. Kubo, Y. Nagahata, M. Ohmura, A. Yachie-Kinoshita, T. Matsuura, T. Morikawa, T. Nakamura, M. Setou, M. Suematsu. Paradoxical ATP elevation in ischemic penumbra revealed by quantitative imaging mass spectrometry. *Antioxid. Redox Signal.* 13: 1157–1167, 2010.
- 9) C. W. Chumbley, M. L. Reyzer, J. L. Allen, G. A. Marriner, L. E. Via, C. E. Barry 3rd, R. M. Caprioli. Absolute quantitative MALDI imaging mass spectrometry: A case of rifampicin in liver tissues. *Anal. Chem.* 88: 2392–2398, 2016.
- 10) B. Prideaux, A. Lenaerts, V. Dartois. Imaging and spatially resolved quantification of drug distribution in tissues by mass spectrometry. *Curr. Opin. Chem. Biol.* 44: 93–100, 2018.
- 11) L. Lamont, D. Hadavi, B. Viehmann, B. Flinders, R. M. A. Heeren, R. J. Vreeken, T. Porta Siegel. Quantitative mass spectrometry imaging of drugs and metabolites: A multiplatform comparison. *Anal. Bioanal. Chem.* 413: 2779–2791, 2021.
- 12) L. Jadoul, R. Longuespee, A. Noel, E. De Pauw. A spiked tissue-based approach for quantification of phosphatidylcholines in brain section by MALDI mass spectrometry imaging. *Anal. Bioanal. Chem.* 407: 2095–2106, 2015.
- 13) P. Källback, T. Vallianatou, A. Nilsson, R. Shariatgorji, N. Schintu, M. Pereira, F. Barre, H. Wadensten, P. Svenningsson, P. E. Andren. Cross-validated matrix-assisted laser desorption/ionization mass spectrometry imaging quantitation protocol for a pharmaceutical drug and its drug-target effects in the brain using time-of-flight and Fourier transform ion cyclotron resonance analyzers. *Anal. Chem.* 92: 14676–14684, 2020.
- 14) R. Legouffe, O. Jeannoton, M. Gaudin, A. Tomezyk, A. Gerstenberg, M. Dumas, C. Heusele, D. Bonnel, J. Stauber, S. Schnebert. Hyaluronic acid detection and relative quantification by mass spectrometry imaging in human skin tissues. *Anal. Bioanal. Chem.* 414: 5781–5791, 2022.
- 15) A. Dannhorn, E. Kazanc, G. Hamm, J. G. Swales, N. Strittmatter, G. Maglennon, R. J. A. Goodwin, Z. Takats. Correlating mass spectrometry imaging and liquid chromatography-tandem mass spectrometry for tissue-based pharmacokinetic studies. *Metabolites* 12: 261, 2022.
- 16) J. A. Barry, R. Ait-Belkacem, W. M. Hardesty, L. Benakli, C. Andonian, H. Licea-Perez, J. Stauber, S. Castellino. Multicenter validation study of quantitative imaging mass spectrometry. *Anal. Chem.* 91: 6266–6274, 2019.
- 17) F. Golpelihi, H. Parastar. Quantitative mass spectrometry imaging using multivariate curve resolution and deep learning: A case study. *J. Am. Soc. Mass Spectrom.* 34: 236–244, 2023.
- 18) K. M. Hines, J. C. May, J. A. McLean, L. Xu. Evaluation of collision cross section calibrants for structural analysis of lipids by traveling wave ion mobility-mass spectrometry. *Anal. Chem.* 88: 7329–7336, 2016.

- 19) N. Takai, Y. Tanaka, K. Inazawa, H. Saji. Quantitative analysis of pharmaceutical drug distribution in multiple organs by imaging mass spectrometry. *Rapid Commun. Mass Spectrom.* 26: 1549–1556, 2012.
- 20) M. R. Groseclose, S. Castellino. A mimetic tissue model for the quantification of drug distributions by MALDI imaging mass spectrometry. *Anal. Chem.* 85: 10099–10106, 2013.
- 21) A. Traberg, F. E. Pinto, A. C. N. Hansen, M. Haedersdal, C. M. Lerche, C. Janfelt. Quantitative mass spectrometry imaging of bleomycin in skin using a mimetic tissue model for calibration. *Pharmaceuticals (Basel)* 15: 1583, 2022.
- 22) J. A. Barry, M. R. Groseclose, S. Castellino. Quantification and assessment of detection capability in imaging mass spectrometry using a revised mimetic tissue model. *Bioanalysis* 11: 1099–1116, 2019.
- 23) S. Shimma, E. Takeo, E. Fukusaki. Protocol for quantitative imaging mass spectrometry. *Bunseki Kagaku* 65: 745–750, 2016 (in Japanese).
- 24) T. Porta, A. Lesur, E. Varesio, G. Hopfgartner. Quantification in MALDI-MS imaging: What can we learn from MALDI-selected reaction monitoring and what can we expect for imaging? *Anal. Bioanal. Chem.* 407: 2177–2187, 2015.
- 25) L. Í. L. Maciel, R. Rodrigues Feitosa Ramalho, R. Izidoro Ribeiro, M. Cunha Xavier Pinto, I. Pereira, B. G. Vaz. Combining the Katritzky reaction and paper spray ionization mass spectrometry for enhanced detection of amino acid neurotransmitters in mouse brain sections. *J. Am. Soc. Mass Spectrom.* 32: 2513–2518, 2021.
- 26) R. Shariatgorji, A. Nilsson, N. Strittmatter, T. Vallianatou, X. Zhang, P. Svenningsson, R. J. A. Goodwin, P. E. Andren. Bromopyrylium derivatization facilitates identification by mass spectrometry imaging of monoamine neurotransmitters and small molecule neuroactive compounds. *J. Am. Soc. Mass Spectrom.* 31: 2553–2557, 2020.
- 27) T. Harada, A. Yuba-Kubo, Y. Sugiura, N. Zaima, T. Hayasaka, N. Goto-Inoue, M. Wakui, M. Suematsu, K. Takeshita, K. Ogawa, Y. Yoshida, M. Setou. Visualization of volatile substances in different organelles with an atmospheric-pressure mass microscope. *Anal. Chem.* 81: 9153–9157, 2009.